Altered distribution of interstitial cells and innervation in the rat urinary bladder following spinal cord injury

Louise Johnston [a], Rebecca M.J. Cunningham [a], John S. Young [b], Christopher H. Fry [b], Gordon McMurray [c], Rachel Eccles [c], Karen D. McCloskey [a], *

[a] Centre for Cancer Research and Cell Biology, School of Medicine, Dentistry and Biomedical Sciences, Queen's University Belfast, Belfast, Northern Ireland, UK
[b] Faculty of Health and Medical Sciences, Wolfson Cell Science Building, University of Surrey, Guildford, Surrey, UK
[c] Pfizer Global Research and Development, Sandwich, Kent, UK

Abstract

Changes in the distribution of interstitial cells (IC) are reportedly associated with dysfunctional bladder. This study investigated whether spinal cord injury (SCI) resulted in changes to IC subpopulations (vimentin-positive with the ultrastructural profile of IC), smooth muscle and nerves within the bladder wall and correlated cellular remodelling with functional properties. Bladders from SCI (T8/9 transection) and sham-operated rats 5 weeks post-injury were used for *ex vivo* pressure–volume experiments or processed for morphological analysis with transmission electron microscopy (TEM) and light/confocal microscopy. Pressure-volume relationships revealed low-pressure, hypercompliance in SCI bladders indicative of decompensation. Extensive networks of vimentin-positive IC were typical in sham lamina propria and detrusor but were markedly reduced post-SCI; semi-quantitative analysis showed significant reduction. Nerves labelled with anti-neurofilament and anti-vAChT were notably decreased post-SCI. TEM revealed lamina propria IC and detrusor IC which formed close synaptic-like contacts with vesicle-containing nerve varicosities in shams. Lamina propria and detrusor IC were ultrastructurally damaged post-SCI with retracted/lost cell processes and were adjacent to areas of cellular debris and neuronal degradation. Smooth muscle hypertrophy was common to SCI tissues. In conclusion, IC populations in bladder wall were decreased 5 weeks post-SCI, accompanied with reduced innervation, smooth muscle hypertrophy and increased compliance. These novel findings indicate that bladder wall remodelling post-SCI affects the integrity of interactions between smooth muscle, nerves and IC, with compromised IC populations. Correlation between IC reduction and a hypercompliant phenotype suggests that disruption to bladder IC contribute to pathophysiological processes underpinning the dysfunctional SCI bladder.

Keywords: bladder • interstitial cell • smooth muscle • nerves • spinal cord injury

Introduction

Spinal cord injury leads to a typical neuropathic bladder exhibiting urinary retention, infections, altered contractility and detrusor-sphincter dyssynergia (DSD). Early stage post-injury is characterized by an areflexic bladder followed by emergence of a spinal micturition reflex enabling limited voiding. Urinary retention, typical in acute and chronic SCI represents a significant clinical problem and is associated with high or low detrusor pressure with the former presenting serious complications such as renal failure. However, low-pressure retention, commonly attributed to reduced detrusor contractility is less amenable to surgical correction and thus persists longer [1, 2]. The pathogenesis of low-pressure retention is unknown and it is important to determine if it is a failure of muscle contractility or a remodelling of tissues within the bladder wall.

The established rat model of neuropathic SCI bladder exhibits time-dependent changes in contractility and compliance coupled with alterations in bladder wall structure [3]. The remarkable complexity that exists within the bladder wall with structural interactions occurring between smooth muscle cells (SMC), nerves, IC,

*Correspondence to: Karen MCCLOSKEY,
Centre for Cancer Research and Cell Biology,
School of Medicine, Dentistry and Biomedical Sciences,
Queen's University Belfast, 97 Lisburn Road,
Belfast BT9 7BL, Northern Ireland, UK.
Tel.: +44-2890-972386
Fax: +44-2890-972776
E-mail: k.mccloskey@qub.ac.uk

Antibody	Supplier	Host	Dilution
Vimentin	Sigma-Aldrich, UK	Goat	1:200
Vimentin (for DAB detection)	Sigma-Aldrich, UK	Mouse	1:200
vAChT	Santa Cruz Biotechnology, USA	Goat	1:200
Neurofilament	Millipore, UK	Mouse	1:200
Anti-goat Alexa 594	Invitrogen, UK	Chicken	1:200

microvessels and the urothelium has been shown over the last decade. The novel IC have attracted particular interest and while their precise roles in bladder physiology have not been fully elucidated, they may modulate bladder smooth muscle activity [4, 5 for recent review]. Interestingly, changes in IC distribution are associated with dysfunctional bladder [6]. Overactive bladder (OAB) mucosal tissue from human and neurogenic rat bladder contain increased Cx43 labelling, associated with lamina propria IC [7, 8] moreover, increased numbers of KIT-positive IC occur in overactive human detrusor [9]. Guinea-pig obstructed bladder exhibits enhanced sub-urothelial and sub-serosal IC [10, 11]. Intriguingly, the underactive, unobstructed, distended bladders typical of megacystis-microcolon intestinal hypoperistalsis syndrome (MMIHS) apparently lack IC [12].

The aim of this study was to evaluate our original hypothesis that 'changes in bladder IC populations following SCI are associated with bladder dysfunction' by (1) investigating the distribution of IC in SCI rat bladder, (2) examining changes in smooth muscle and innervation post-SCI and (3) correlating the morphological findings with compliance, evaluated by *ex vivo* pressure–volume experiments.

Materials and methods

Rat SCI model

Protocols complied with European Community Council Directive 86/609/EEC and French legislation under a French Ministry license to Neureva (France). Bladders from adult female Sprague-Dawley rats post-SCI (T8 laminectomy, isoflurane anaesthesia 2% in O_2, 0.6 L/min) or sham-operated controls (shams) were obtained from Neureva. Animals were assisted with bladder voiding for 2 weeks by abdominal compression twice daily until micturition reflexes emerged and were injected daily, for the first week with gentamicin (2 mg/kg). After 5 weeks, rats were weighed, killed by cervical dislocation and exsanguination; the bladders were removed, weighed and stored in Ca^{2+}-free Krebs at 4°C. Data are expressed as mean ± S.E.M.; statistical comparisons were made using Student's unpaired *t*-test with significance accepted at $P < 0.05$.

Pressure–volume relationships

Whole SCI and sham bladders were catheterized, *ex vivo*, and ligated around the urethra and bladder neck. Bladders were filled (Minipuls3; Gilson, Middleton, WI, USA) at 12 ml/hr with Ca^{2+}-free Krebs, until pressure remained stable or when leakage around the catheter was observed. Intravesical pressure and volume were recorded (Spike 2; CED, Cambridge, UK). Composition of Ca^{2+}-free Krebs solution: NaCl 114 mM, KCl 4.7 mM, $MgSO_4$ 1.2 mM, KH_2PO_4 1.2 mM, $NaHCO_3$ 25 mM, glucose 11.7 mM; gassed with 95% O_2/5% CO_2).

Immunohistochemistry and electron microscopy

Bladders were opened longitudinally and pinned to the Sylgard base of a dissecting dish. The mucosal layer containing urothelium and lamina propria was removed by sharp dissection to leave the underlying detrusor layer. Mucosal and detrusor tissue sheets were labelled with antibodies as previously described [13] and imaged with confocal microscopy (Nikon C1). Control tissues were prepared by (1) omission of all antibodies to control for autofluorescence; (2) omission of the primary antibody to control for non-specificity of the secondary antibody and (3) guinea-pig bladder was used as a positive control. Details of the antibodies used are shown in Table 1. Cell counts were made by two independent, blinded researchers on reconstructed z-stacks from non-overlapping fields of view. Vimentin-positive IC with at least two cytoplasmic projections from a central cellular soma were counted for each field of view and expressed per unit area (100 μm^2). Images from slides stained with anti-neurofilament or anti-vAChT were reconstructed as z-stacks in Image J (NIH, Bethesda, MD, USA) software, the background was subtracted, image intensity (integrated density) was measured and expressed per 100 μm^2. Data are expressed as mean ± S.E.M.; comparisons were made with Mann-Whitney test with significance accepted at $P < 0.05$.

Tissues fixed in 8% neutral buffered formalin were processed for wax histology. Sections (5 μm) were deparaffinized in xylene, rehydrated in alcohol, washed in tap water and heated (pressure cooker) in Tris-EDTA (pH 9.0) for antigen retrieval. Endogenous peroxidase activity was blocked with 3% H_2O_2, sections were washed, blocked with 1% BSA in Tris buffer solution (TBS) and incubated in anti-vimentin overnight. Sections were then washed in TBS, incubated in rabbit antimouse horseradish peroxidase conjugate (1:200), washed, stained with diaminobenzidine tetrahydrochloride (DAB) and substrate chromogen system (DAKO, Cambridgeshire, UK) before counterstaining with haematoxylin (Autostainer, Leica) and viewing with light microscopy.

Bladders removed from sham ($N = 3$) and SCI ($N = 3$) rats immediately after killing were processed for TEM as previously described [14].

Results

Animals ($N = 21$ in each group) were weighed before surgery and pre-sacrifice. *Ex vivo* bladders were weighed post-sacrifice (Fig. 1). Significant differences were not found in animal mass pre-surgery (229.9 ± 2.3 g sham *versus* 230.4 ± 2.5 g SCI, $P = 0.87$); however, post-surgery SCI animals were significantly lighter than
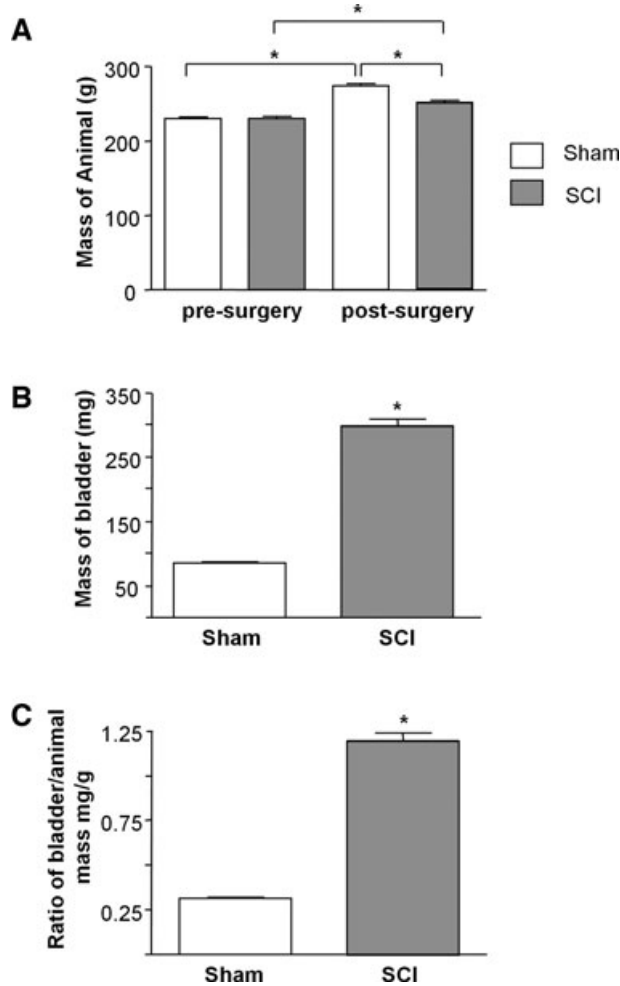
Fig. 1 Effect of spinal cord transection on animal and bladder mass. (**A**) Summary data from sham operated and spinal cord injured animals ($N = 21$ in each group) showing significant increase in body mass in both groups after the 5-week intervention period and a significant difference in body mass post-surgery between sham and SCI animals. (**B**) The bladders of SCI animals had significantly greater mass than sham animals post-surgery ($N = 21$, $P < 0.05$). (**C**) Bladder to body mass ratio was significantly higher in the SCI group compared with sham-operated controls ($P < 0.05$).

shams (249.5 ± 2.8 g *versus* 274.4 ± 2.4 g, $P < 0.0001$, respectively). SCI bladders were significantly heavier than shams (298.3 ± 11.0 mg *versus* 85.7 ± 1.6 mg, $P < 0.0001$), moreover the bladder-to-body mass ratio was significantly larger in SCIs (0.31 ± 0.01 sham *versus* 1.19 ± 0.04 SCI, $P < 0.001$).

Pressure–volume relationships

Bladders were filled at a constant rate and the corresponding pressure changes recorded. Differences in the pressure–volume
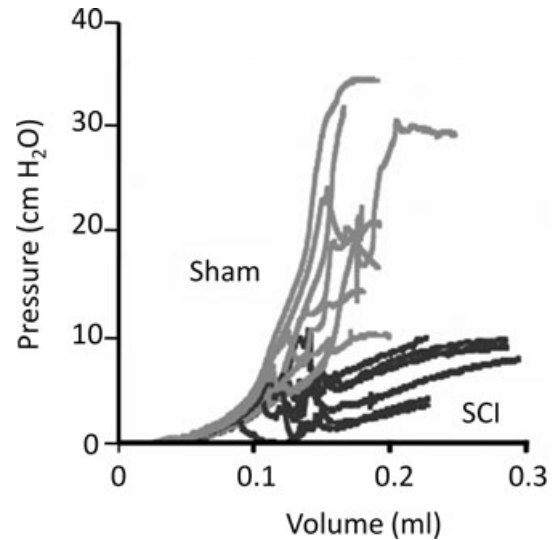

Fig. 2 Pressure–volume relationships. Pressure–volume curves of *ex vivo* bladders showing continuous pressure tracings as a function of filling volume. Data are from sham-operated controls (grey) and SCI animals (black). A reduction of slope indicates increased compliance.

relationships (Fig. 2) between sham controls and SCI bladders indicated that SCI bladders were more compliant than shams. Compliance was calculated from the secondary, linear part of pressure–volume relationships and was greater in SCI bladders (26.5 ± 4.7 μl/cmH$_2$O, $N = 8$, mean $\pm$ S.D.) compared to control (2.9 ± 0.9 μl/cmH$_2$O, $N = 9$).

Immunohistochemical evaluation of IC

Tissue sections from sham bladders ($N = 3$) had extensive vimentin staining throughout the lamina propria (Fig. 3A) and detrusor; surrounding the muscle bundles and occupying inter-bundle spaces (Fig. 3C and E). SCI bladders ($N = 3$) had reduced vimentin staining in both lamina propria (Fig. 3B) and detrusor (Fig. 3D and F); stained cells had a rounded morphology compared with shams. Smooth muscle hypertrophy was evident in SCI micrographs.

Whole-mount preparations of sham mucosa imaged with confocal microscopy showed networks of stellate-shaped, vimentin-positive cells (Fig. 4A and B), however SCI tissues had rounded cells, with truncated cellular branches which appeared unable to form networks (Fig. 4C). Dense networks of vimentin-positive stellate-shaped cells and elongated, bipolar cells at the edge of smooth muscle bundles, were found in sham detrusors (Fig. 5A, C and E). SCI detrusors had a striking reduction in vimentin-positive cells, containing only small patches of non-networked cells (Fig. 5B, D and F). At higher magnification, vimentin-positive cells in SCI detrusors lacked branched processes, becoming rounded or unipolar. Semi-quantitative analysis showed that
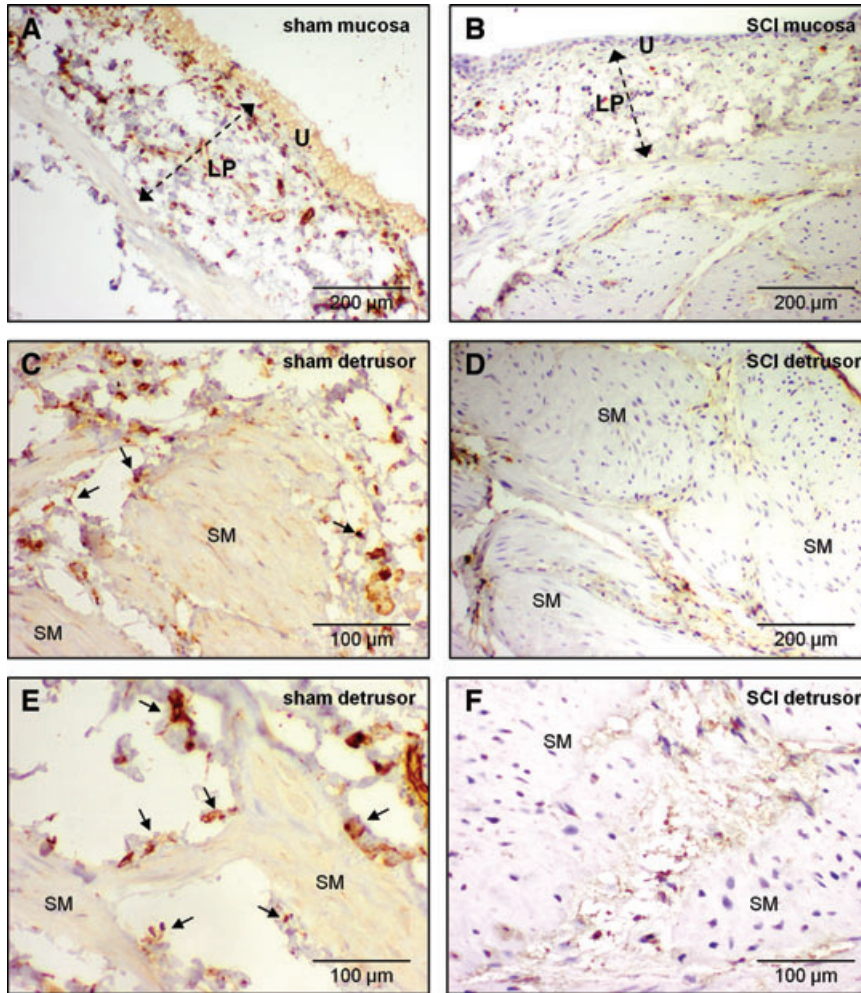
Fig. 3 Vimentin immunohistochemistry in histological sections. (**A**) Abundant vimentin-positive cells stained with DAB (brown) in a mucosal section of sham rat bladder. Lamina propria (LP), urothelium (U). Sections were counterstained with haematoxylin. (**B**) Vimentin-positive cells were less abundant in the lamina propria of SCI bladder. Staining was predominantly in rounded, cell bodies compared with the cellular structures seen in (**A**). (**C**, **E**) Vimentin-positive cells in the detrusor were found on the boundary (arrows) of smooth muscle bundles (SM) and in the inter-bundle spaces of sham bladders. (**D**, **F**) In SCI detrusor, vimentin-positive cells were notably less abundant and had a compromised (rounded) cellular morphology. Note the hypertrophied smooth muscle in SCI compared with sham bladders.

vimentin-positive cells within the bladder wall (per 100 μm^2) were significantly reduced from 3.7 ± 0.3 in shams ($n = 86$ micrographs from $N = 6$ bladders) to 0.4 ± 0.07 in SCIs ($n = 65$ micrographs from $N = 6$ bladders; $P < 0.0001$).

Visualisation of bladder nerves

The neuronal plexus labelled with anti-neurofilament found in sham lamina propria was markedly reduced post-SCI (Fig. 6A and B). Fluorescence intensity (arbitrary units per 100 μm^2) was reduced from 26,771 ± 2621 in shams ($n = 18$ micrographs, $N = 3$ bladders) to 12,777 ± 2150 ($n = 14$ micrographs, $N = 3$ bladders). Dense innervation in sham detrusor, typified by large nerve trunks bifurcating and becoming progressively smaller became regions of patchy denervation alongside morphologically disrupted nerves post-SCI (Fig. 6C and D). Neurofilament labelling

was reduced from 33,165 ± 1967 in shams ($n = 24$, $N = 3$) to 18,273 ± 1596 after SCI ($n = 25$; $N = 3$; $P < 0.001$. Abundant cholinergic nerve varicosities (vesicular–acetylcholine–transferase labelling) typical of sham detrusor (22,631 ± 843, $n = 16$; $N = 2$) were markedly reduced in SCIs (15,950 ± 1139, $n = 16$; $N = 2$; Fig. 7). Summary data are shown in Figure 7E.

Transmission electron microscopy

TEM revealed differences in the ultrastructural integrity of components of the bladder wall between shams and SCIs. Cells with the typical ultrastructural profile of bladder IC (discontinuous basal lamina, central nuclei, lateral branches, rough and smooth endoplasmic reticulum, mitochondria, caveolae and cytoplasmic vesicles; Refs. [14] and [15]) were abundant in the lamina propria of shams with frequent IC–IC

Fig. 4 Confocal imaging of vimentin-positive cells in lamina propria. (**A**, **B**) Whole mount, flat sheet preparations of sham bladder mucosa were labelled with anti-vimentin and imaged with confocal microscopy. All images are reconstructions of optical sections. Networks of vimentin-positive cells were found in the lamina propria. Vimentin-positive cells had bipolar or highly branched stellate morphology. (**C**) Mucosal tissues from SCI animals also had vimentin-positive cells however, the networks were apparently less well developed than the sham operated controls and cells had a compromised, non-branched morphology. (**D**) Tissues labelled with only the secondary antibody (primary antibody omitted) had minimal staining.
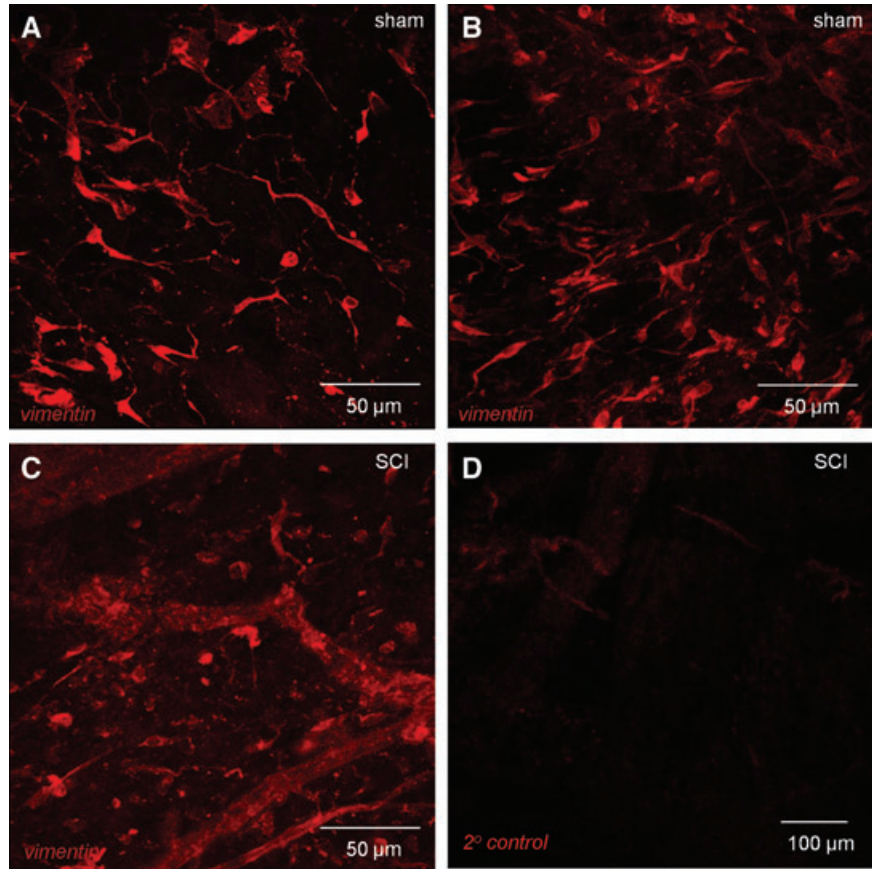
contacts (Fig. 8A and B). Recent publications indicate that tissues may contain cells distinct from fibroblasts, myofibroblasts or interstitial cells of Cajal (ICC), termed 'telocytes' [16, 17]. Telocytes have been defined as having multiple cell projections, which are very thin (less than 0.2 μm), characteristically long (may be >100 μm) and having multiple dilations and caveolae. It is possible that the IC described in this study may encompass telocytes although their presence in bladder has not yet been reported. Lamina propria IC post-SCI had fewer cellular associations and a retraction/loss of cell branches was evident (Fig. 8C and D).

Sham detrusor (Fig. 9A–D) contained IC, which were frequently associated with nerve varicosities and SMC; significantly, IC made close contacts with nerve varicosities. Neuronal structures were either missing or too difficult to identify due to degradation in SCIs (Fig. 9E–H), which typically contained areas of cellular debris. Moreover, SMC also showed a degree of degradation. IC cell bodies, exhibiting significant degradation were found in the detrusor, these were more difficult to find post-SCI, consistent with the reduction in vimentin-positive cells seen in confocal micrographs. Ultrastructurally, damaged IC exhibited cytoplasmic vacuolization, swollen endoplasmic reticulum, apparent collapse of the cytoskeleton in the perinuclear area and some swollen mitochondria.

Discussion

The human SCI bladder exhibits early (acute) and late (chronic) changes in function, also exhibited by the spinal cord transected (T8/9 or T9/10) rat. After the acute areflexic phase, chronic SCI bladders develop voiding reflexes attributed to new spinal cord reflexes [18], which enable limited voiding. Simultaneous contraction of detrusor and urethral smooth muscle (detrusor-sphincter dyssynergia) however, results in urinary retention, increased workload on the bladder and subsequent bladder hypertrophy [3]. This study focussed on the chronic SCI rat bladder, which is reported to have increased compliance and structural changes including smooth muscle hypertrophy [19, 20]. Functional experiments demonstrated that the SCI bladders in the present study had the hypercompliant phenotype typical of chronic SCI.
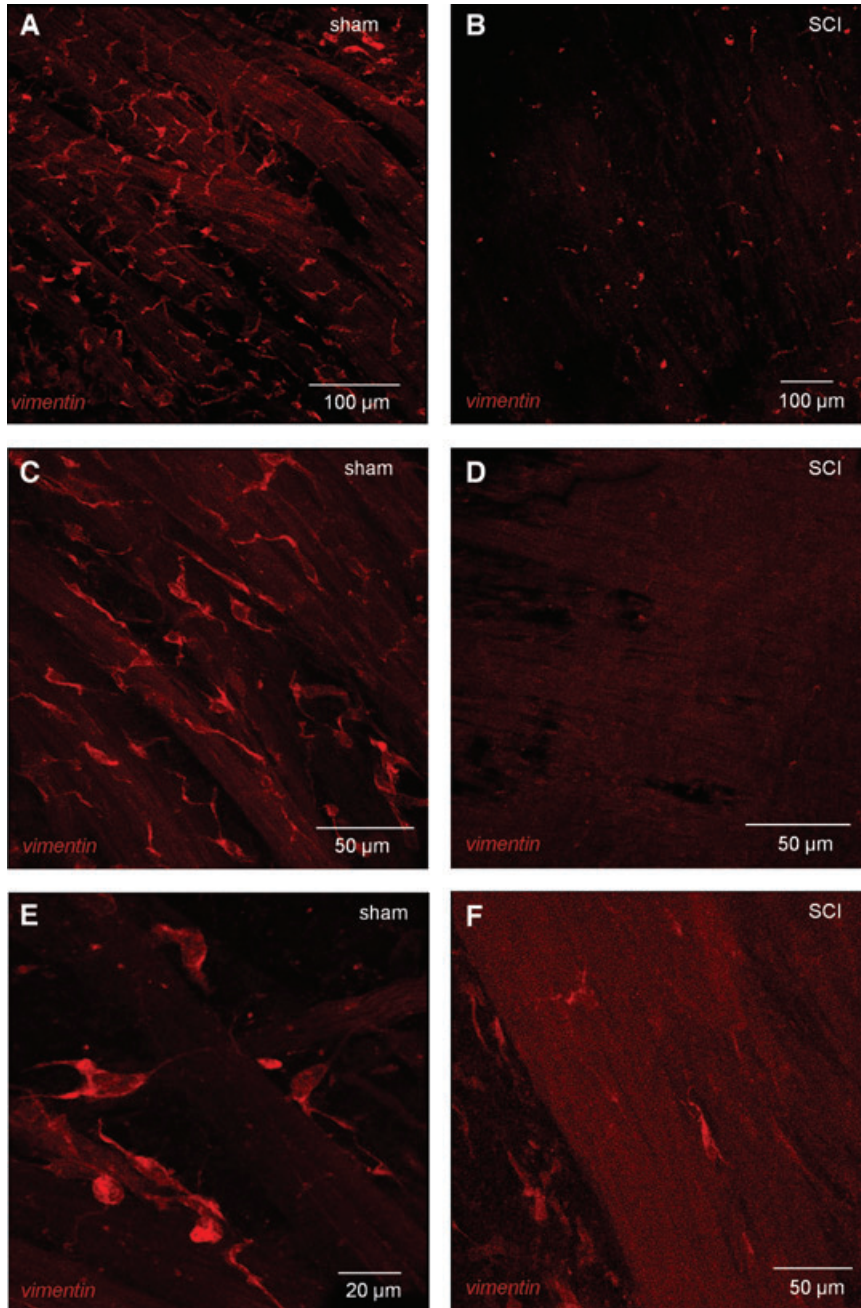
Fig. 5 Vimentin-positive cells in the detrusor of sham and SCI bladders. (**A**) Whole mount, flat sheet preparations of sham detrusor were labelled with anti-vimentin and imaged with confocal microscopy. All images are reconstructions of optical sections. Vimentin-positive cells formed extensive networks in the detrusor. (**C**, **E**) At higher magnification, the immunopositive cells had a highly branched stellate morphology and occupied the spaces between the smooth muscle bundles. Vimentin-positive cells were also found on the boundary of the smooth muscle bundles either bipolar cells, orientated axially or stellate cells spanning two or more bundles as shown in panel C. (**B**, **D**, **F**). Vimentin-positive cells were markedly altered in SCI tissues with only a few patches of cells visible, which generally had lost their stellate morphology.

Interestingly, chronic SCI led to a marked reduction in IC sub-populations, labelled with the broad IC marker, anti-vimentin [13, 15, 21], which had been abundant in shams. Lamina propria IC may have been less affected than detrusor IC but their distribution and morphology were clearly altered post-SCI. TEM confirmed that IC cell bodies were present in the lamina propria post-SCI but that their morphological integrity and structural connections were compromised. The remarkable near-absence of IC in confocal images of post-SCI detrusor was confirmed with TEM which demonstrated occasional, ultrastructurally damaged IC. The ultrastructural damage to the bladder IC which included swollen mitochondria, cytoplasmic vacuolisation, enlarged endoplasmic reticulum is reminiscent of that reported for gastrointestinal ICC in Crohn's disease [22]. Recent evidence

Fig. 6 Confocal imaging of bladder neural networks. (**A**) Whole mount, flat sheet preparations of mucosa from sham bladders were labelled with anti-neurofilament and imaged with confocal microscopy. All images are reconstructions of optical sections. A neural plexus was observed in these sections comprising larger nerves, which bifurcated to increasingly smaller fibres. (**B**) In SCI animals, the neural plexus was significantly disrupted with an apparent reduction in nerves. (**C**) The detrusor region of sham control bladders was densely innervated with large nerve trunks subdividing into increasingly smaller nerves, which became varicosities (arrows) within the smooth muscle bundles. Mucosal tissues from SCI animals also had strikingly compromised neuronal distribution with only occasional patches of immunopositive nerves. (**D**) In SCI detrusor, the innervation was comparatively sparse with only patchy areas of nerves visible.
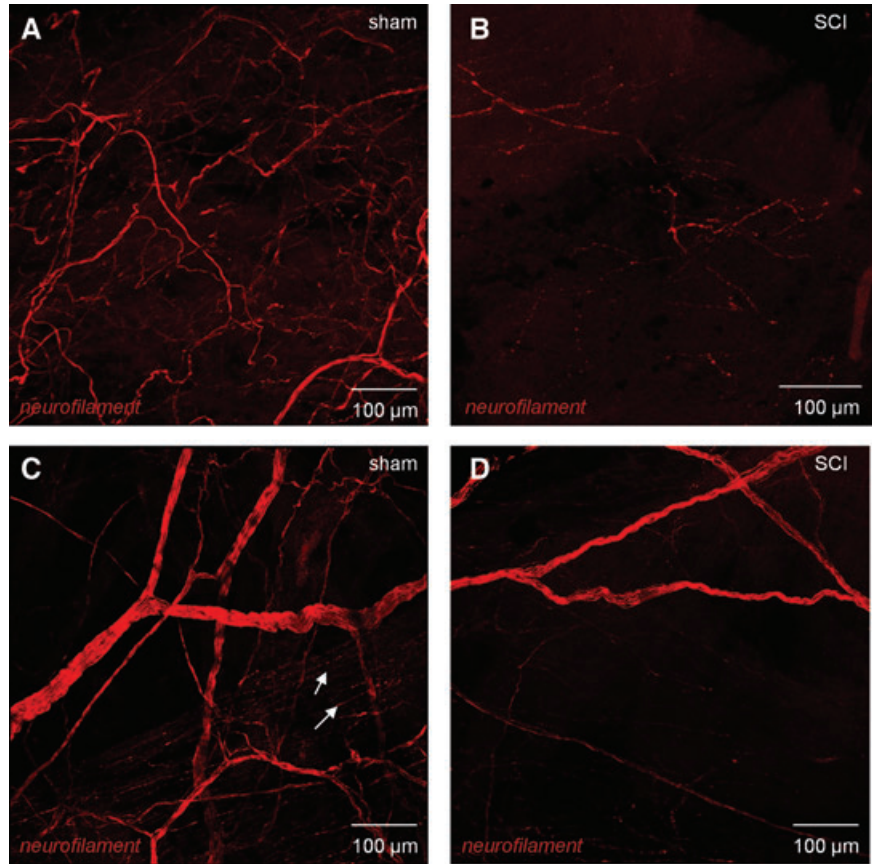
supports a correlation between numbers of IC and bladder activity in pathophysiological conditions [6]. Increased sub-urothelial and sub-serosal IC in (overactive) obstructed guinea-pig bladder [10, 11] and a lack of IC in the non-contractile bladders of patients with MMIHS has been reported [12]. Increased Cx43 expression in rat mucosa 4 weeks post-SCI [7] and in neurogenic or idiopathic OABs [8, 23] may indicate up-regulation in numbers of Cx43-positive IC. Biers *et al.* [9] reported increased KIT-positive IC in human neuropathic detrusor. If IC modulate detrusor activity in normal bladder and their up-regulation correlates with an OAB phenotype, then their loss in the low-pressure, hypercompliant chronic SCI bladder in this study would be consistent with a decompensated phenotype.

The patchy denervation observed in this study is in agreement with findings from human neurogenic (NDO) bladder biopsies [24, 25]. Axonal degeneration observed by TEM in human NDO biopsies, notably exceeded the degree of smooth muscle degeneration within the same biopsy [26, 27]. We also found remarkable areas of degeneration and cell debris throughout the detrusor (where neuronal structures would be typically located) adjacent to SMC, which themselves showed a degree of degeneration. Post-SCI

decreases in vAChT-immunoreactivity in pelvic ganglia and bladder wall nerves have been reported to recover, accompanied with improvement in bladder function [28]. However, the significant decrease in detrusor vAChT varicosities post-SCI in this study indicated that at 5 weeks post-injury, recovery was incomplete. A link between innervation and maintenance of the IC phenotype has been demonstrated in gut where anterograde degeneration of vagal afferent innervation resulted in a concomitant degeneration of IC and nerves [29]. This may indicate that release of a neuronal trophic factor is necessary for maintenance of the IC phenotype; interestingly, stem cell factor, the natural ligand of the IC KIT receptor is present in gastrointestinal nerves [30]. This study demonstrated close synaptic-like contacts between nerve varicosities and IC in sham bladders, which were not detected post-SCI likely due to nerve degeneration and reductions in IC. These findings may suggest that bladder IC rely on neuronal release of trophic factors, for example KIT for their maintenance.

Alternative explanations for IC degeneration post-SCI may be related to detrusor SMC hypertrophy linked with increased levels of the neurotrophin, nerve growth factor (NGF). Increased mRNA and protein expression of NGF in chronic SCI rat bladder is
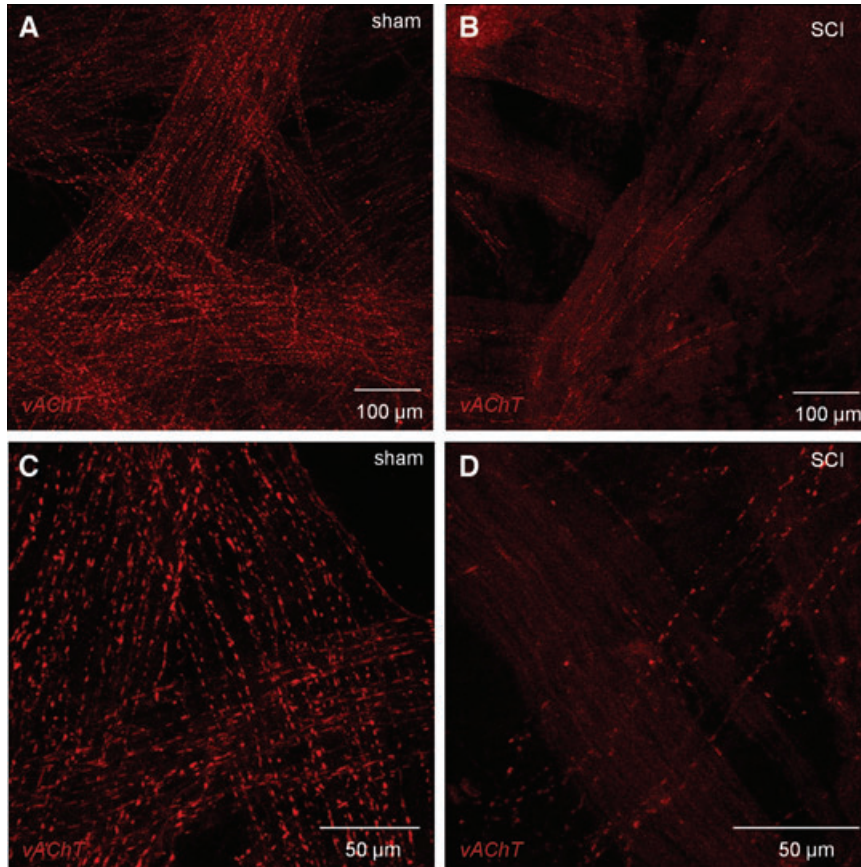
Fig. 7 Confocal imaging of cholinergic nerves. (**A**, **C**) Whole mount, flat sheet preparations of sham detrusor were labelled with anti-vesicular acetylcholine-transferase (vAChT) and imaged with confocal microscopy. All images are reconstructions of optical sections. A dense cholinergic innervation was clear within the detrusor. (**B**, **D**) SCI detrusor had marked reduction in vAChT varicosities. (**E**) Summary graph of the effect of spinal cord injury on vAChT-positive nerves in the detrusor ($n = 16$ micrographs from $N = 2$ bladders, Sham and SCI groups), neurofilament-positive nerves in the mucosa ($n = 18$, $N = 3$ sham; $n = 14$, $N = 3$ SCI) and detrusor ($n = 24$, $N = 3$ sham; $n = 25$, $N = 3$ SCI). The asterisk indicates $P < 0.05$.
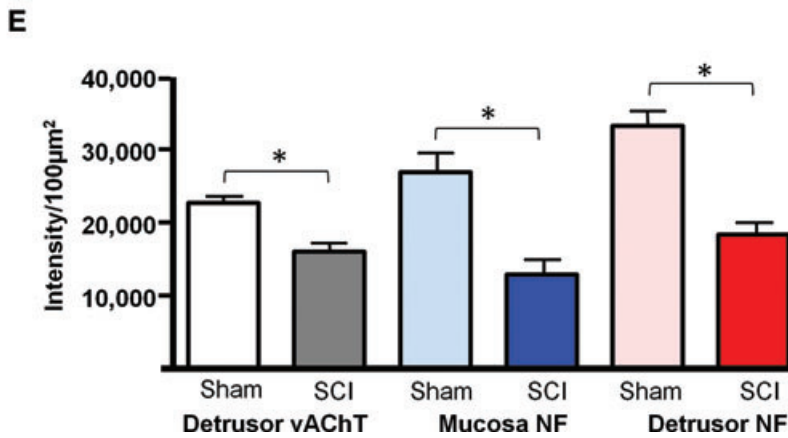
associated with bladder hypertrophy [18] moreover, NGF is released from bladder SMC *in vitro* following mechanical stretch [31, 32]. The association between bladder hypertrophy and increased NGF is common to bladder pathophysiologies including SCI, bladder inflammation/cystitis and urethral obstruction [33].

Interestingly, intrathecal neutralisation of NGF improved bladder function in SCI rats [34]. Taken together, hypertrophied smooth muscle in response to chronic SCI-induced DSD could release NGF resulting in IC degeneration. If so, our findings may indicate that NGF is an anti-survival factor for IC maintenance.
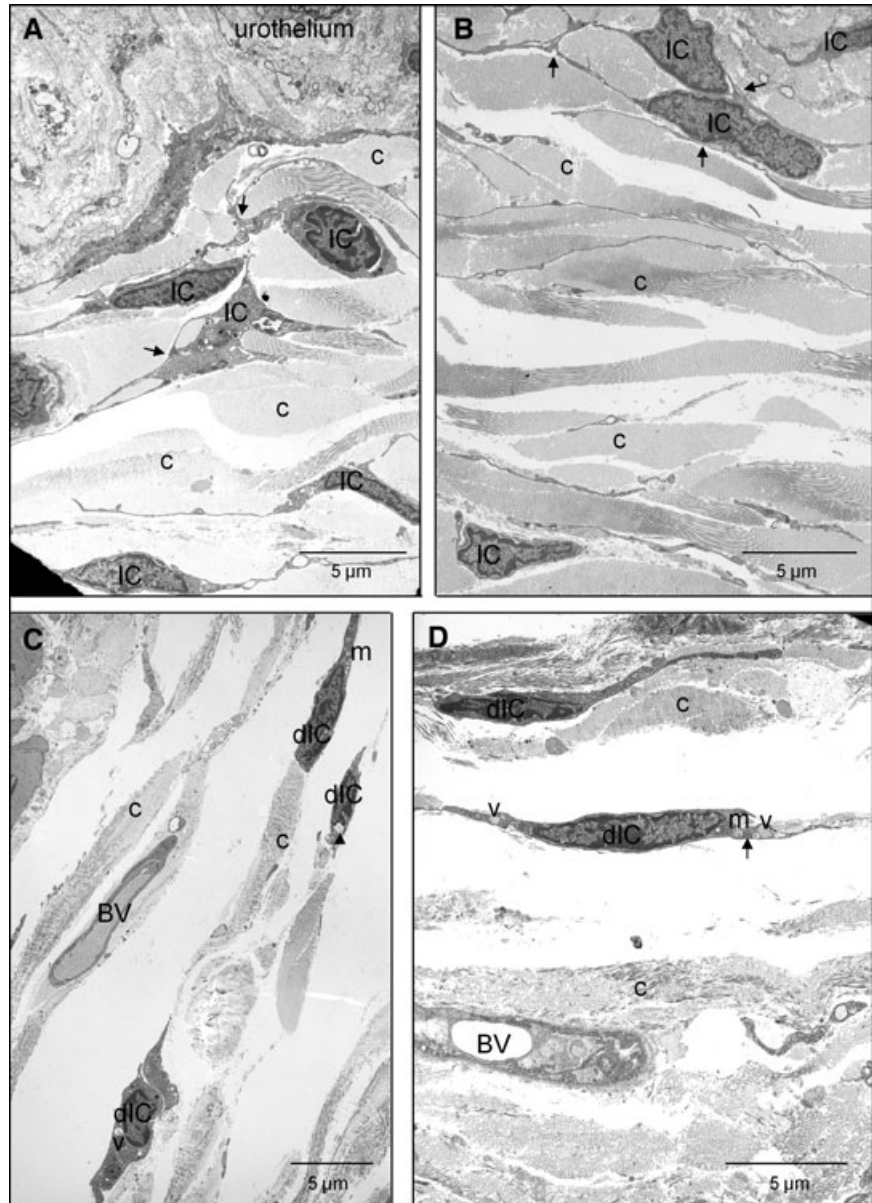
Fig. 8 Transmission electron micrographs of lamina propria IC in sham and SCI bladders. (**A**, **B**) The lamina propria region of sham bladders had abundant cells with the ultrastructural properties of IC. Cell–cell interactions are shown by arrows and collagen was abundant (c). The base of the urothelium is visible. (**C**, **D**) After SCI, damaged IC (dIC) were apparent, although their branched process and cell–cell contacts were less extensive than sham controls. dIC typically had cytoplasmic vacuolisation (v), swollen endoplasmic reticulum (arrows), apparent collapse of the cytoskeleton in the perinuclear area (arrowheads) and some swollen mitochondria (m). Blood vessels are visible (BV).

Conclusions

The novel finding that IC populations are significantly decreased in chronic SCI bladders corroborates the link between the morphology and distribution of IC and bladder activity indicating that IC loss is correlated with a low-pressure, hypercompliant phenotype. Extensive remodelling of the bladder wall occurring at this stage post-injury is also characterized by neuronal degradation and smooth muscle hypertrophy. We propose that the IC loss may be explained by decreased pro-survival factors and increased anti-survival factors related to smooth muscle and neuronal adaptations.
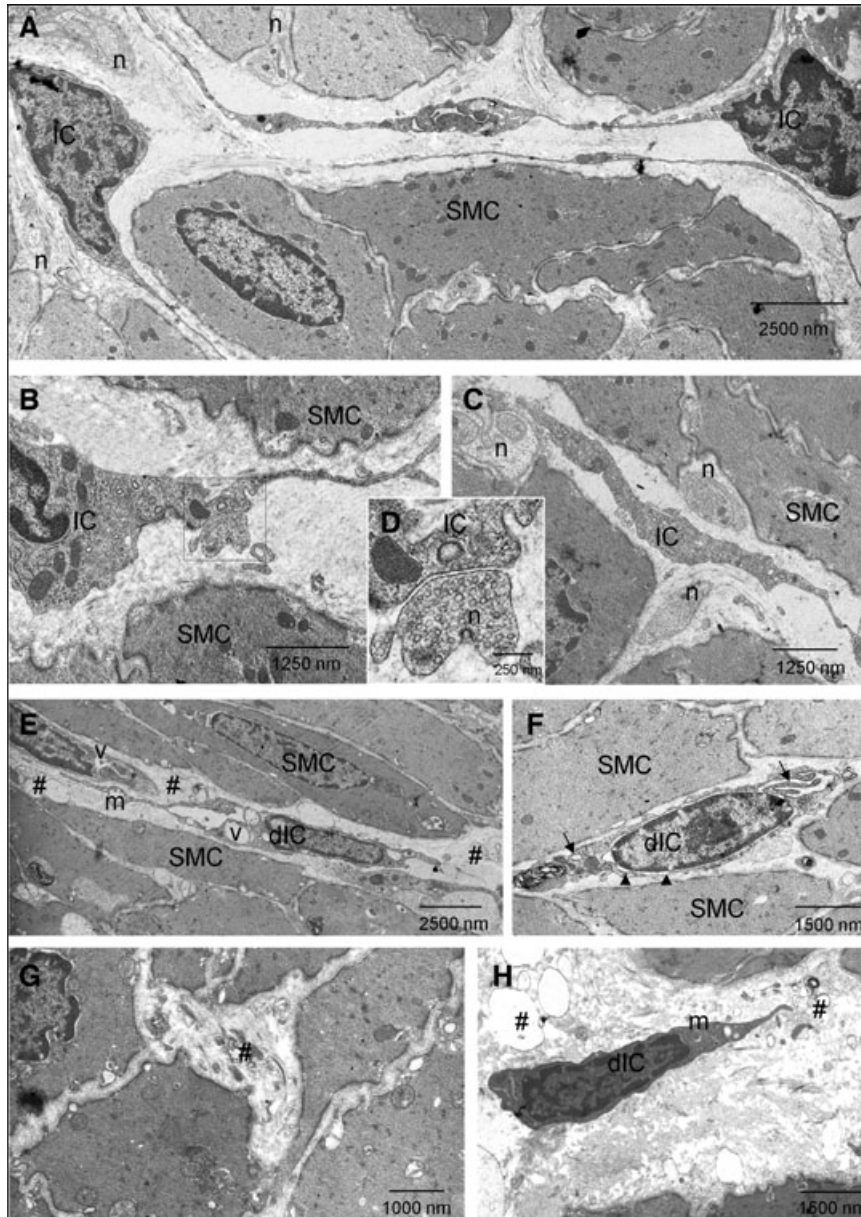
Acknowledgements

Fig. 9 Transmission electron micrographs of detrusor IC in sham and SCI bladders (**A–C**) Cells with ultrastructural characteristics of IC were present in sham detrusors. These had cytoplasmic branches and were close to smooth muscle cells (SMC). Nerve (n) varicosities were abundant and were in close contact with both SMC and IC. (**D**) Magnification of the boxed area in B showing synapse-like contact between an IC and a nerve ending. (**E–H**) After SCI, damaged IC (dIC) were present with evidence of damage to branched processes and cell–cell contacts. dIC typically had cytoplasmic vacuolisation (v), swollen endoplasmic reticulum (arrows), apparent collapse of the cytoskeleton in the perinuclear area (arrowheads) and some swollen mitochondria (m). Areas of cellular debris were abundant (#). SMC exhibited a lesser degree of degradation.

Authors' Contributions

Conception and design of study KDMcC, CHF, RE
Data Acquisition LJ, JSY, RMJC
Data analysis, interpretation LJ, JSY, RMJC, KDMcC, CHF
Manuscript drafting KDMcC
Critical revision of manuscript KDMcC, CHF, LJ, JSY
Statistical analysis KDMcC, LJ, JSY

Obtained funding KDMcC, CHF, RE, GMcM
Supervision KDMcC, CHF, RE, GMcM

Conflict of interest

The authors confirm that there are no conflicts of interest.

References

1. **Abrams PH, Dunn M, George N.** Urodynamic findings in chronic retention of urine and their relevance to results of surgery. *Br Med J.* 1978; 2: 1258–60.

2. **Kalejaiye O, Speakman MJ.** Management of acute and chronic retention in men. *Eur Urol.* 2009; 8: 523–9.

3. **Cruz C, Cruz F.** Spinal cord injury and bladder dysfunction: new ideas about an old problem. *Scientific World J.* 2011; 11: 214–34.

4. **McCloskey KD.** Interstitial cells of Cajal in the urinary tract. *Handb Exp Pharmacol.* 2011a; 202: 233–54.

5. **Hashitani H, Lang RJ.** Functions of ICC-like cells in the urinary tract and male genital organs. *J Cell Mol Med.* 2010; 14: 1199–211.

6. **McCloskey KD.** Interstitial cells and bladder pathophysiology-passive bystanders or active participants? *J Urol.* 2011b; 185: 1562–3.

7. **Ikeda Y, Fry C, Hayashi F, et al.** Role of gap junctions in spontaneous activity of the rat bladder. *Am J Physiol Renal Physiol.* 2007; 293: F1018–25.

8. **Roosen A, Datta SN, Chowdhury RA, et al.** Suburothelial myofibroblasts in the human overactive bladder and the effect of botulinum neurotoxin type A treatment. *Eur Urol.* 2009; 55: 1440–8.

9. **Biers SM, Reynard JM, Doore T, et al.** The functional effects of a c-kit tyrosine inhibitor on guinea-pig and human detrusor. *BJU Int.* 2006; 97: 612–6.

10. **Kubota Y, Hashitani H, Shirasawa N, et al.** Altered distribution of interstitial cells in the guinea pig bladder following bladder outlet obstruction. *Neurourol Urodyn.* 2008; 27: 330–40.

11. **Grol S, Nile CJ, Martinez-Martinez P, et al.** M(3) Muscarinic receptor-like immunoreactivity in sham operated and obstructed guinea pig bladders. *J Urol.* 2011; 185: 1959–66.

12. **Piaseczna Piotrowska A, Rolle U, Solari V, et al.** Interstitial cells of Cajal in the human normal urinary bladder and in the bladder of patients with megacystis-microcolon intestinal hypoperistalsis syndrome. *BJU Int.* 2004; 94: 143–6.

13. **Davidson RA, McCloskey KD.** Morphology and localization of interstitial cells in the guinea pig bladder: structural relationships with smooth muscle and neurons. *J Urol.* 2005; 173: 1385–90.

14. **Cunningham RM, Larkin P, McCloskey KD.** Ultrastructural properties of interstitial cells of Cajal in the Guinea pig bladder. *J Urol.* 2011; 185: 1123–31.

15. **Sui GP, Rothery S, Dupont E, et al.** Gap junctions and connexin expression in human suburothelial interstitial cells. *BJU Int.* 2002; 90: 118–29.

16. **Popescu LM, Faussone-Pellegrini MS.** TELOCYTES-a case of serendipity: the winding way from Interstitial Cells of Cajal (ICC), *via* Interstitial Cajal-Like Cells (ICLC) to TELOCYTES. *J Cell Mol Med.* 2010; 14: 729–40.

17. **Cantarero Carmona I, Luesma Bartolomé MJ, Junquera Escribano C.** Identification of telocytes in the lamina propria of rat duodenum: transmission electron microscopy. *J Cell Mol Med.* 2011; 15: 26–30.

18. **Vizzard MA.** Changes in urinary bladder neurotrophic factor mRNA and NGF protein following urinary bladder dysfunction. *Exp Neurol.* 2000; 161: 273–84.

19. **Toosi KK, Nagatomi J, Chancellor MB, et al.** The effects of long-term spinal cord injury on mechanical properties of the rat urinary bladder. *Ann Biomed Eng.* 2008; 36: 1470–80.

20. **Nagatomi J, Toosi KK, Grashow JS, et al.** Quantification of bladder smooth muscle orientation in normal and spinal cord injured rats. *Ann Biomed Eng.* 2005; 33: 1078–89.

21. **Smet PJ, Jonavicius J, Marshall VR, et al.** Distribution of nitric oxide synthase-immunoreactive nerves and identification of the cellular targets of nitric oxide in guinea-pig and human urinary bladder by cGMP immunohistochemistry. *Neuroscience.* 1996; 71: 337–48.

22. **Wang XY, Zarate N, Soderholm JD, et al.** Ultrastructural injury to interstitial cells of Cajal and communication with mast cells in Crohn's disease. *Neurogastroenterol Motil.* 2007; 19: 349–64.

23. **Haferkamp A, Mundhenk J, Bastian PJ, et al.** Increased expression of connexin 43 in the overactive neurogenic detrusor. *Eur Urol.* 2004; 46: 799–805.

24. **Drake MJ, Gardner BP, Brading AF.** Innervation of the detrusor muscle bundle in neurogenic detrusor overactivity. *BJU Int.* 2003; 91: 702–10.

25. **Drake MJ, Hedlund P, Mills IW, et al.** Structural and functional denervation of human detrusor after spinal cord injury. *Lab Invest.* 2000; 80: 1491–9.

26. **Haferkamp A, Dörsam J, Resnick NM, et al.** Structural basis of neurogenic bladder dysfunction. III. Intrinsic detrusor innervation. *J Urol.* 2003a; 169: 555–62.

27. **Haferkamp A, Dörsam J, Resnick NM, et al.** Structural basis of neurogenic bladder dysfunction. II. Myogenic basis of detrusor hyperreflexia. *J Urol.* 2003b; 169: 547–54.

28. **Takahara Y, Maeda M, Nakatani T, et al.** Transient suppression of the vesicular acetylcholine transporter in urinary bladder pathways following spinal cord injury. *Brain Res.* 2007; 1137: 20–8.

29. **Huizinga JD, Reed DE, Berezin I, et al.** Survival dependency of intramuscular ICC on vagal afferent nerves in the cat esophagus. *Am J Physiol Regul Integr Comp Physiol.* 2008; 294: R302–10.

30. **Torihashi S, Yoshida H, Nishikawa S, et al.** Enteric neurons express Steel factor-lacZ transgene in the murine gastrointestinal tract. *Brain Res.* 1996; 738: 323–8.

31. **Persson K, Sando JJ, Tuttle JB, et al.** Protein kinase C in cyclic stretch-induced nerve growth factor production by urinary tract smooth muscle cells. *Am J Physiol.* 1995; 269: C1018–24.

32. **Tanner R, Chambers P, Khadra MH, et al.** The production of nerve growth factor by human bladder smooth muscle cells *in vivo* and *in vitro. BJU Int.* 2000; 85: 1115–9.

33. **Steers WD, Tuttle JB.** Mechanisms of disease: the role of nerve growth factor in the pathophysiology of bladder disorders. *Nat Clin Pract Urol.* 2006; 3: 101–10.

34. **Seki S, Sasaki K, Fraser MO, et al.** Immunoneutralization of nerve growth factor in lumbosacral spinal cord reduces bladder hyperreflexia in spinal cord injured rats. *J Urol.* 2002; 168: 2269–74.